HOSTED BY

ELSEVIER

Available online at www.sciencedirect.com

ScienceDirect

Journal of Radiation Research and Applied Sciences

journal homepage: http://www.elsevier.com/locate/jrras

Experimental and simulated study of detector collimation for a portable 3″ × 3″ NaI(Tl) detector system for *in-situ* measurements

K.U. Kiran [a,*], *K. Ravindraswami* [b], *K.M. Eshwarappa* [a], *H.M. Somashekarappa* [c]

[a] *Government Science College, Hassan 573 201, Karnataka, India*

[b] *St Aloysius College (Autonomous), Mangalore 575 003, Karnataka, India*

[c] *University Science Instrumentation Centre, Mangalore University, Mangalagangothri, 574 199 D K, Karnataka, India*

ARTICLE INFO

Article history:
Received 12 May 2015
Received in revised form
29 June 2015
Accepted 21 July 2015
Available online 7 August 2015

Keywords:
Saturation thickness
Collimation
Signal-to-noise ratio
Multiple scattering fraction
Scintillation detector

ABSTRACT

The effect of detector collimator and scatterer thickness on multiple Compton back-scattered gamma photons is studied. Gamma photons from a ^{137}Cs source of 5.8 mCi, is allowed to fall on Carbon, Aluminium, Iron and Copper targets and the scattered photons are detected by a properly shielded 76 mm × 76 mm NaI(Tl) scintillation detector located at 90° to the incident beam. To extract the contribution of multiple scattered photons from the measured spectra, single scattered distribution is remodelled analytically. The thickness at which the multiple scattered photons saturate is determined for different detector collimator apertures and scatterer thicknesses. The variation of saturation thickness, Signal-to-Noise (S/N) ratio, Multiple Scattering Fraction (MSF) for different materials and collimator sizes are studied and compared with the available literature. Monte Carlo simulated calculations using MCNP code supports the present experimental work.

1. Introduction

Gamma backscattering method is one of the widely used non-destructive evaluation (NDE) techniques to evaluate materials. The material under investigation and the detector system under the same plane makes gamma backscattering technique as one of the major advantages over the transmission method. Because of the low cost and high efficiency, the NaI(Tl) detectors have become very popular among variety of gamma detectors. The light weight feature of the integrated, compact NaI(Tl) detector are very much suitable for *in-situ* measurements. Several researchers across the world have used NaI(Tl) detectors for *in-situ* measurements in underwater, road transport inspection, forest, building materials, soil and mineral samples (Bezuidenhout, 2013; Golosov et al., 2000; Jaquiel, Carlos, & Avacir, 2010; Kovler et al., 2013; Kwang, In, Sung-Woo, & Ho-Sik, 2008; Plamboeck, Nylen, & Agren, 2006; Povinec, Osvath, & Baxter, 1996; Vlachos & Tsabaris, 2005; Vrba & Fojtik, 2014).

* *Corresponding author*. Tel.: +91 9483032052.
E-mail address: kirangsch@gmail.com (K.U. Kiran).

Peer review under responsibility of The Egyptian Society of Radiation Sciences and Applications.
http://dx.doi.org/10.1016/j.jrras.2015.07.006

Compton scattering is observed when photons interact with the matter of low Z elements in the energy range of 0.1–10 MeV. This is an inelastic scattering where photon collides with the unbound electron of the atom. Due to the finite dimension of the target, photon suffers scattering many times, which leads to multiple scattering. The quantification of multiple scattering of photons is helpful in assessment of Compton profiles, radiation shielding and industrial tomography. Using this method, our previous work successfully assigned effective atomic number to composite materials (Ravindraswami, Kiran, Eshwarappa, & Somashekarappa, 2014).

Literature survey on multiple scattering shows many used either Monte Carlo simulations or analytical methods to find the multiple scattering contributions, but experimental and simulated work for the same geometrical set up are not available. Due to complex nature of the scattering and differing geometrical restrictions, analytical approaches (Dumond, 1930; Halonen & Williams, 1979; Kirkpatrick, 1937; Tanner & Epstein, 1976) to the study of multiple scattering usually cannot provide all the information of the scattering. Hence Monte Carlo methods were generally used to predict the multiple scattering. Monte Carlo simulation work was carried out to find multiple scattering contamination in Compton scattering studies, where simulations were made as a function of the photon energy (60–662 keV), for the atomic number of the scatterer (Z = 6–38) and the collimation geometry (Pitkanen, Cooper, Laundy, & Holt, 1987). The contribution of multiple scattering in cement blocks (with holes and iron intrusions) were studied during backscattering studies using EGS4 simulation (Shengli, Jun, & Liuxing, 2000). The validity of the Monte Carlo simulations with the experiments, single and multiple scattered photon profiles and related parameters is necessary to correct the contaminations. Monte Carlo studies (Felsteiner, Pattison, & Cooper, 1974; Tanner & Epstein, 1976) relate multiple scattering to the sample thickness. The energy and intensity as a function of angular distribution for 662 keV multiple scattered photons from the materials of different Z and thickness confirmed that the contribution of multiple scattered radiations increases with target thickness (Singh, Singh, Sandhu, & Singh, 2008).

The experimental work on the study of effect of collimator size and target thickness contributions on multiple scattering showed that saturation thickness doesn't get altered by collimator size of the detector (Arvind, Sandhu, & Singh, 2009; Singh, Singh, Sandhu, & Singh, 2006). The multiple scattering parameters like signal-to-noise ratio and MSF are also explained for the cylindrical samples of aluminium using 0.662 MeV gamma photons for the scattering angles of 90° and 180° respectively. The effect of multiple scattered photons in the measurement of attenuation coefficient of composite materials can be minimized by using a well collimated narrow beam geometry (Sidhu, Singh, Singh, & Mudahar, 1999). The work also showed that by reducing the collimator size the effect of multiple scattered photons can be neglected even up to a large absorber thickness (Gurdeep, Karamjit, Parjit, & Gurmel, 1999). More recently it was observed that mass attenuation coefficients values decreases with increasing detector collimator diameter (Celik, Cevik, & Celik, 2012). The effect of collimator size and absorber thickness on gamma-ray attenuation measurements of sandy and clayey soils was investigated, optimization of collimator size is found essential (Costa, Borger, & Pires, 2014). Therefore it is very much required to study the variation of scattered photons, multiple scattered photons, signal-to-noise ratio and MSF as a function of collimation sizes.

The present paper describes the experimental study of different detector collimators and sample thickness on multiple backscattered gamma rays using ^{137}Cs gamma source. Carbon, aluminium, iron and copper scatterers are used and the scattered photons are detected by a properly shielded 76 mm × 76 mm NaI(Tl) scintillation detector located at 90° to the incident beam. The source scatterer distance and source detector distances are kept constant. The saturation thickness, signal-to-noise ratio and MSF are studied. Monte Carlo calculation performed using Monte Carlo N-Particle (MCNP) code and the experimental results are compared.

2. Experimental set-up

Fig. 1 shows the diagram of the experimental set-up for the measurement of scattered γ-rays. For the present measurements, gamma photons are obtained from the radioactive source of ^{137}Cs of strength 5.8 mCi. The ^{137}Cs source is in the form of capsule sealed in an aluminium tube of thickness 20 mm and length 115 mm. The active portion of the source is 10 mm in thickness and 6 mm in length. In order to minimize the background effects of radiation, the active portion of source is shielded using a cylindrical lead ring of thickness 50 mm and a diameter of 160 mm. The source shielding, detector shielding and collimation are obtained using cylindrical lead rings of 50 mm thickness. In addition to this, 4 cylindrical lead rings (120 mm diameter and 50 mm thickness) were specially prepared to enclose the source both from the back and the front sides. The gamma ray spectrometer consists of 76 mm × 76 mm NaI(Tl) scintillation detector. The distance of scatterer from source collimator is kept 220 mm so that angular spread due to source collimator (15 mm) on the target is ±1.9°. The distance of source can be varied up to 430 mm from the scatterer center.

The detector crystal is covered with an aluminium window of 0.8 mm thick and optically coupled to photo-multiplier tube. To avoid the contribution due to background radiations the detector is shielded by cylindrical lead shielding of length

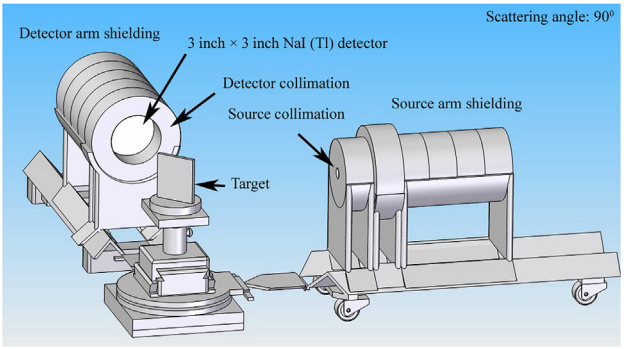

Fig. 1 – Experimental set-up.

200 mm, thickness of 35 mm and internal diameter of 90 mm. Because of the low cost, easy availability and good attenuation for gamma photons, lead was used to shield the source and the detector. The use of lead shielding for the source generates K X-rays in the range of 20–100 keV. In order to avoid these background radiations and increase the signal-to-noise ratio, the inner side of the shielding is covered with 2 mm thick iron and 3 mm thick aluminium with iron facing towards lead Raghunath, Bhatnagar, and Meenakshisundaram (1983). The distance of source can be varied up to 400 mm and the distance of detector can be varied up to 270 mm from the scatterer center. The distance of the scatterer from the detector is kept 262 mm so that the angular spread due to the detector collimator (74 mm) on the target is ±8.1°. The entire experimental set-up was placed at a height of 340 mm on a sturdy wooden table. This table was placed in the center of the room to minimize scattering from the walls of the room. The source-detector assembly is arranged in such a way that the centres of source collimator and gamma ray detector pass through the center of scatterer.

3. Method of measurements

The gamma ray spectrometer consists of a 76 mm × 76 mm NaI(Tl) scintillation detector. The experimental data were accumulated on a PC based gamma spectrometer with a fully integrated multichannel analyser (MCA). The Microsoft Windows-XP based spectroscopic application software *winTMCA32* acted as a user interface for system set-up and display. All gamma ray spectral functional adjustments were synchronized through this application software. A software program using *winTMCA32* was written for the present experimental set-up in order to evaluate parameters such as Full Width Half Maximum (FWHM), multiple scattering events and single scattering events.

The schematic diagram of the experimental set-up is shown in Fig. 2. The backscattered photons from the scatterer are measured by the NaI(Tl) scintillation detector located at an angle of 90°. This experimental spectrum consists of both single and multiple scattered counts. The multiple scattered counts are obtained from the measured spectrum by remodelling single scattered spectrum. By referring to Fig. 3, let I_0 be the incident gamma photons having energy E_0 from the ^{137}Cs source to the object of thickness x_0. During scattering, the energy of gamma photons reduces to E within the target dx at a distance x and scattering angle of θ_1.

The number of photons $n(E,x)$ scattered within a thickness element dx at a distance x in the scatterer at an angle θ_1 degraded to energy E, emerging out of the scatterer and reaching the detector is given by

$$n(E,x) = I_0 \alpha dx n_e e^{-\mu_1 x} \left[\frac{d\sigma}{d\Omega}\right]_{\theta_1} e^{-\mu_2 r} d\Omega_1 \quad (1)$$

where α is the cross-section area of the incident beam, n_e is number of electrons/cm^3 in the medium. The quantities μ_1 and μ_2 are total attenuation coefficients of scattering medium at energies E_0 and E_1, respectively. XCOM software provides values of total attenuation coefficients for a given atomic number at desired photon energy (Berger et al., 2010). $\left[\frac{d\sigma}{d\Omega}\right]_{\theta_1}$ is the Klein–Nishina cross-section at an angle θ_1 and $d\Omega_1$ is the solid angle subtended by the detector at scattering point of scatterer. Here $r = AB$, $\theta_1 = \theta + x/r_0 \sin\theta$ where $r_0 = \theta_1 - \theta$ and $d\Omega_1 = \pi a^2/[r_0 + x\sec(\pi - \theta_1)]^2$ where a is the radius of the detector collimator. From Fig. 3 it is clear that with increase in thickness of scatterer, θ remains the same, but θ_1 goes on changing. Due to spread in scattering angle corresponding to different points in target along direction of propagation of primary gamma beam, photons scattered at various points in scatterer contribute to scattered energy that goes on changing. The scattered photon energy is given by familiar Compton relation:

$$E = \frac{E_0}{1 + \frac{E_0}{m_0 c^2}(1 - \cos\theta_1)} \quad (2)$$

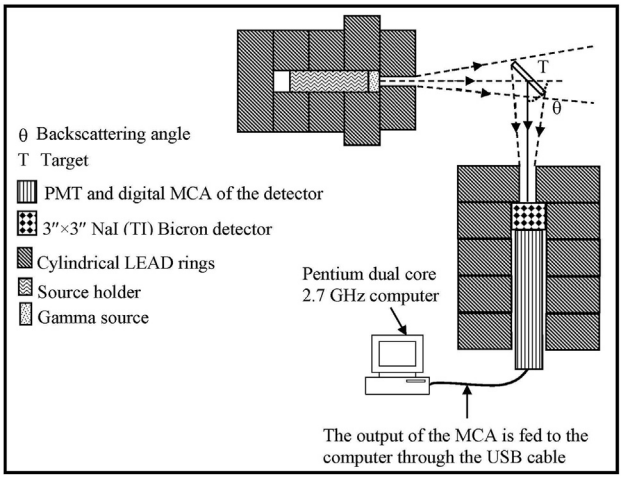

Fig. 2 – Schematic diagram of the experimental set-up.

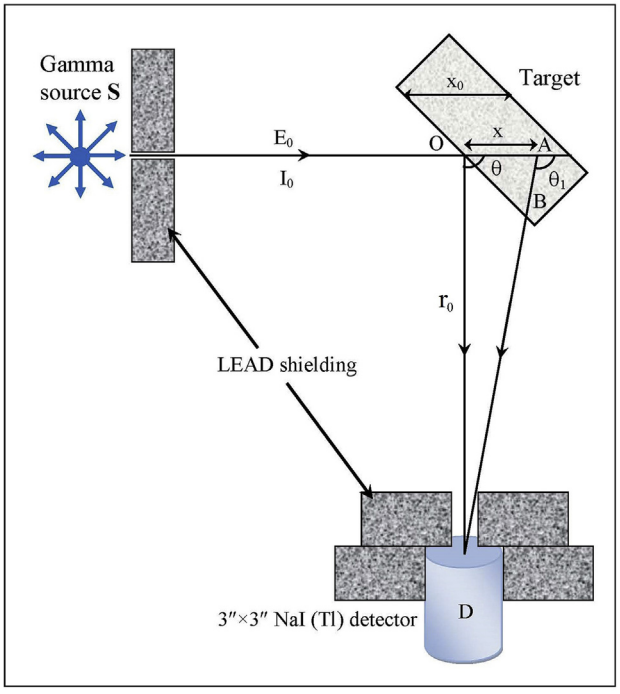

Fig. 3 – Scattering process of the experimental set-up.

By considering these facts, values of $n(E,x)$ at any energy E are calculated for different values of x, θ_1 and corresponding to different values of scattered energies E. The total number of photons scattered from sample can be found by evaluating the integral

$$n(E) = \frac{1}{x_0}\int n(E,x),dx \tag{3}$$

When incident on the detector, $n(E)$ gives rise to a pulse height distribution whose full-energy peak at energy E can be represented by a Gaussian distribution $Y(E)$ with an area given by

$$A = n(E)\varepsilon_i(E)\left(\frac{P}{T}\right)_E \tag{4}$$

where $\varepsilon_i(E)$ is total detection efficiency of crystal and $(P/T)_E$ is peak to total ratio at the energy E (Crouthamel, Adams, & Dams, 1970). Gaussian distribution can be written as

$$Y(E) = Y_0 e^{-\frac{(E-E_0)^2}{b}} \tag{5}$$

where $b = \Delta E/4\ln 2$, Y_0 is normalization constant and ΔE is FWHM of detector corresponding to energy E. Area under Gaussian peak can be represented as $A = 1.064Y_0\Delta E$.

Using the number of counts at peak position Y_0 and *FWHM* of the detector, the number of photons of the Gaussian distribution $Y(E)$ for each energy E can be calculated. The total number of photons at desired energy is obtained by numerically integrating $Y(E)$. This results in an analytically estimated single scattered spectrum as registered by the detector. Normalization at the maximum peak results in the contribution of single scattered photons. Total intensity of the single scattered photons is then obtained by dividing normalized peak area by photo-fraction. In order to obtain multiple scattered photons, the analytically reconstructed single scattered distribution is subtracted from the experimental noise corrected composite spectrum (Kiran, Ravindraswami, Eshwarappa, & Somashekarappa, 2014; Paramesh, Venkataramaiah, Gopala, & Sanjeeviah, 1983; Singh et al., 2006; Singh, Singh, Sandhu, & Singh, 2007a, 2007b).

4. Results and discussions

4.1. *Method of data acquisition*

Backscattered spectrum is obtained by irradiating scatterer using the ^{137}Cs source for 1000 s (Plot-a of Fig. 4). In order to have a full exposure of the target under study, each target material were of the parallelepiped shape with a dimension of 100 mm × 100 mm × 10 mm. The scatterer is then removed to find the background or noise spectrum, which is also recorded for the same period of time to permit registration of events unrelated to the target (Plot-b of Fig. 4). Noise subtracted spectrum (Plot-c of Fig. 4) is obtained by subtracting noise spectrum (Plot-b of Fig. 4) from backscattered spectrum (Plot-a of Fig. 4). Plot-c of Fig. 4 consists of both single and multiple scattered events. Plot-d of Fig. 4 is the analytically reconstructed single scattered spectrum that is obtained from the values of maximum counts of the noise subtracted spectrum

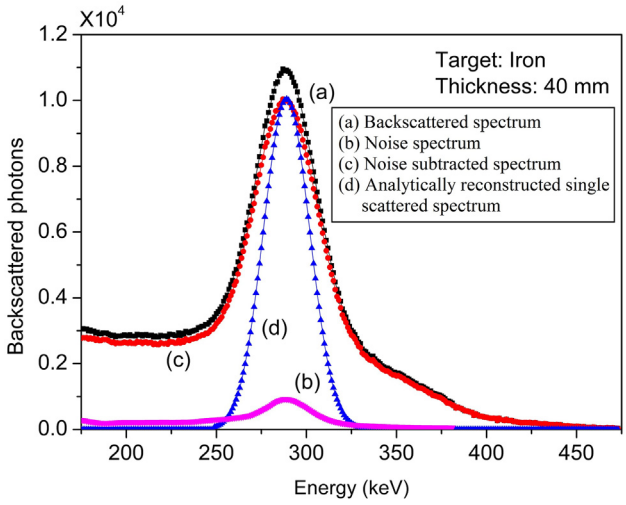

Fig. 4 – A typical experimentally observed spectrum (Curve-a) with 40 mm thick iron target. An observed background spectrum (Curve-b) without target in the primary beam. Background subtracted events (Curve-c). Normalized analytically reconstructed single scattered spectrum (Curve-d).

and FWHM of the detector system. Subtraction of reconstructed single scattered spectrum from noise subtracted spectrum in the region of interest (ROI) energy range results in only multiple scattered photons. This procedure is repeated for varies thicknesses of the material and for other materials also.

4.2. *Multiple scattered photons and saturation thickness of the scatterer*

Fig. 5 displays the experimental multiple scattered photons as a function of thickness of the targets for various collimators opening. For each of the detector collimation, each plot show that for an increase in sample thickness there is an increase in multiple scattering intensity and then it becomes almost a constant. The thickness of the sample above which the multiple scattering intensity remains almost constant is termed the "saturation thickness". Due to the increase in target thickness, the number of photons undergoing multiple scattering increases. However, after a certain thickness, the probability of absorption within the sample retards multiple-scattering. Hence there exists equilibrium of multiple scattering and absorption within the target, thereby saturating the intensity of photons leaving the target. The value of saturation thicknesses for Carbon, Aluminium, Iron and Copper are 125 mm, 70 mm, 31 mm and 25 mm respectively. We observed that the saturation thickness for materials is independent of the variation in detector collimator size. Hence saturation thickness is independent of detector collimator aperture for a given material.

4.3. *Experimental and MCNP simulated data comparison*

The experimentally obtained scattered photons for a collimator size of 75 mm and the MCNP simulation obtained

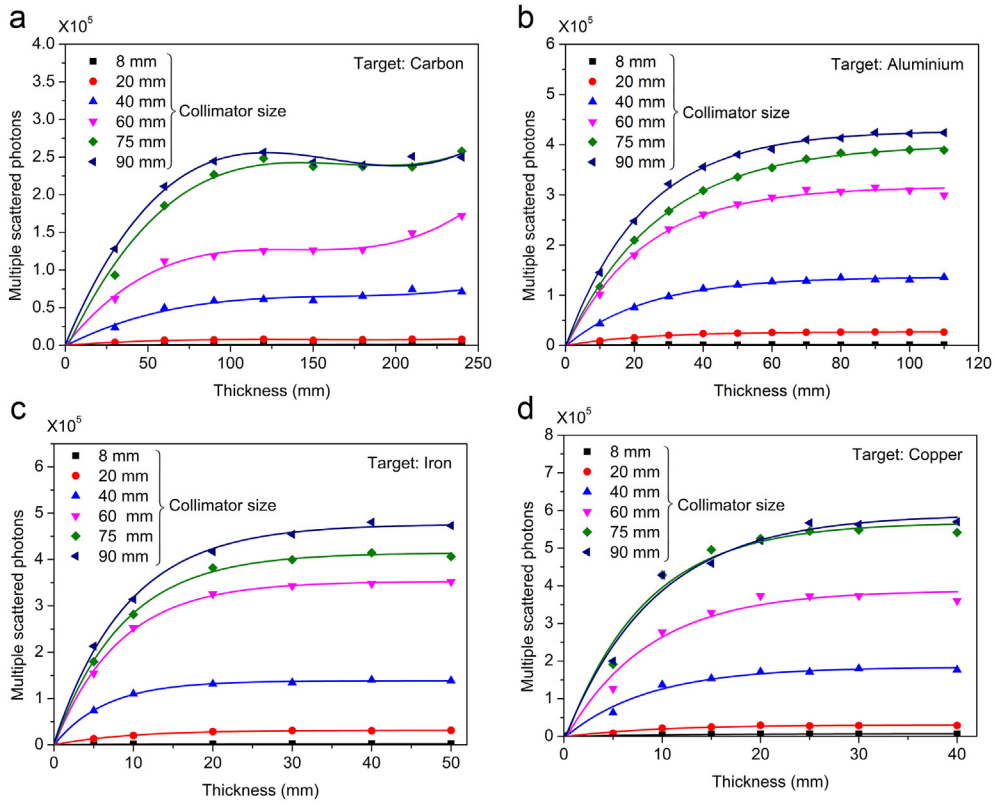

Fig. 5 – Experimental variation of multiple scattered photons as a function of target thickness for various collimator sizes for different materials.

scattered photos are plotted as a function of target thickness for various materials and is shown in Fig. 6. The plots show a good agreement with the experimental and simulated values.

4.4. *Effect of detector collimator aperture on multiple scattered photons*

The experimental study was carried out using 6 collimators of diameters 8 mm, 20 mm, 40 mm, 60 mm, 75 mm and 90 mm to the scintillation detector. For a particular collimator size, the thickness of the target materials (Carbon, Aluminium, Iron and Copper) were increased till the saturation thickness and little further. The multiple scattered photons for the 4 materials are obtained with respect to detector collimator size and scatterer thickness.

Fig. 7 displays the plot of multiple scattered photons as a function of collimator sizes for various target thicknesses for Carbon, Aluminium, Iron and Copper respectively. The collimator size is normalized to the diameter of the detector's crystal. The plots in these figures show that the number of multiple scattered events increases with increase in the diameter of detector collimator. For small scatterer thickness the increase in the intensity of multiple scattered photons for an increase in collimator size is lesser because of less probability for multiple scattering. As the scatterer thickness increases, the intensity of multiple scattered photons increases to a higher value with increase in detector collimator size as compared to thin targets. For a collimation size of less than 0.8, there is a lesser variation in the number of multiple scattered events, but beyond this thickness and collimator size there is sudden increase in the multiple scattered photons. The sudden increase in the multiple scattered photons is due to the fact that the rise in the solid angle subtended by the detector as the collimator opening increases. Hence the contribution of multiple scattered photons found from more volume of the targets, which increases the acceptance angle at the detector front face. This increase in the number of multiple scattered photons is observed up to saturation thickness of the target.

4.5. *Signal-to-noise ratio*

In Compton profiles and cross-section measurements only the single scattered photons are desired and the multiple scattered photons act as background noise to the original signal. The ratio of number of single scattered events to number of multiple scattered events known as signal-to-noise ratio is plotted as a function of target thickness for different collimator apertures (Fig. 8). When the target thickness is large, the signal-to-noise ratio is low indicating the presence of more multiple scattered photons in comparison to the single scattered events. If multiple scattering backgrounds are to be avoided, a high signal-to-noise ratio is must, which can be obtained by using very thin targets. From the plots it is evident that for large size of detector collimation the signal-to-noise ratio is low. This indicates the presence of more multiple scattered photons when compared to single scattered photons. The signal-to-noise ratio can be increased by decreasing

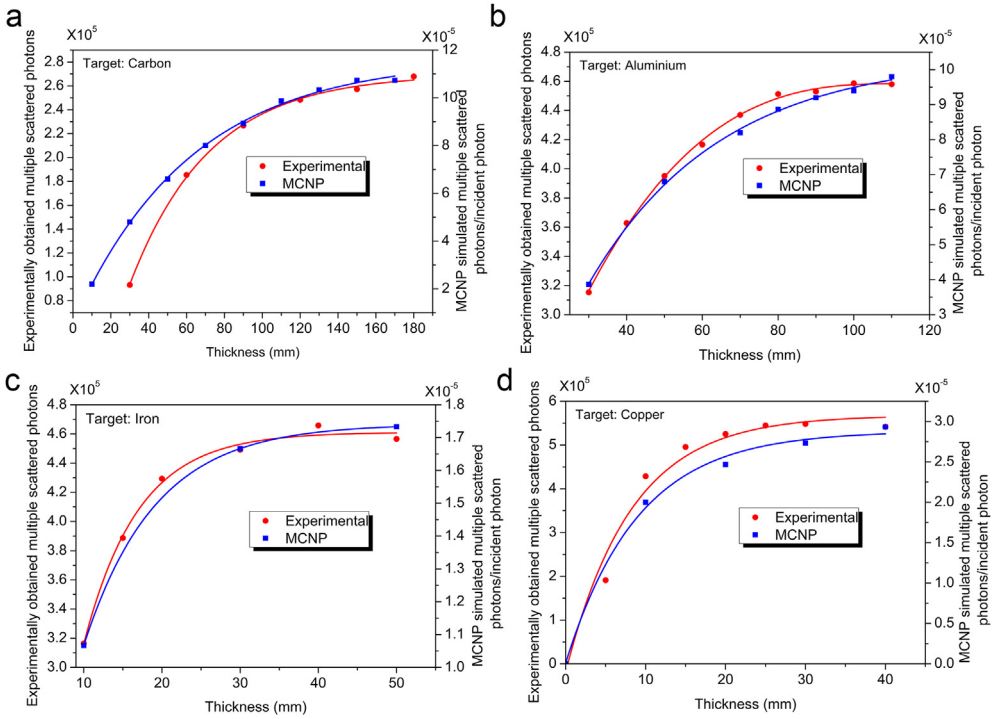

Fig. 6 – An inter-comparison of experimental (for a collimator size of 75 mm) and MCNP simulated data.

the multiple scattering photons. This is possible if narrow detector collimation and thin targets are used. This is in good agreement with the Monte Carlo calculations work (Shengli et al., 2000) and the experimental work (Singh et al., 2006).

4.6. *MSF*

The single scatter component of the backscattered radiation provides the information about the object structure in

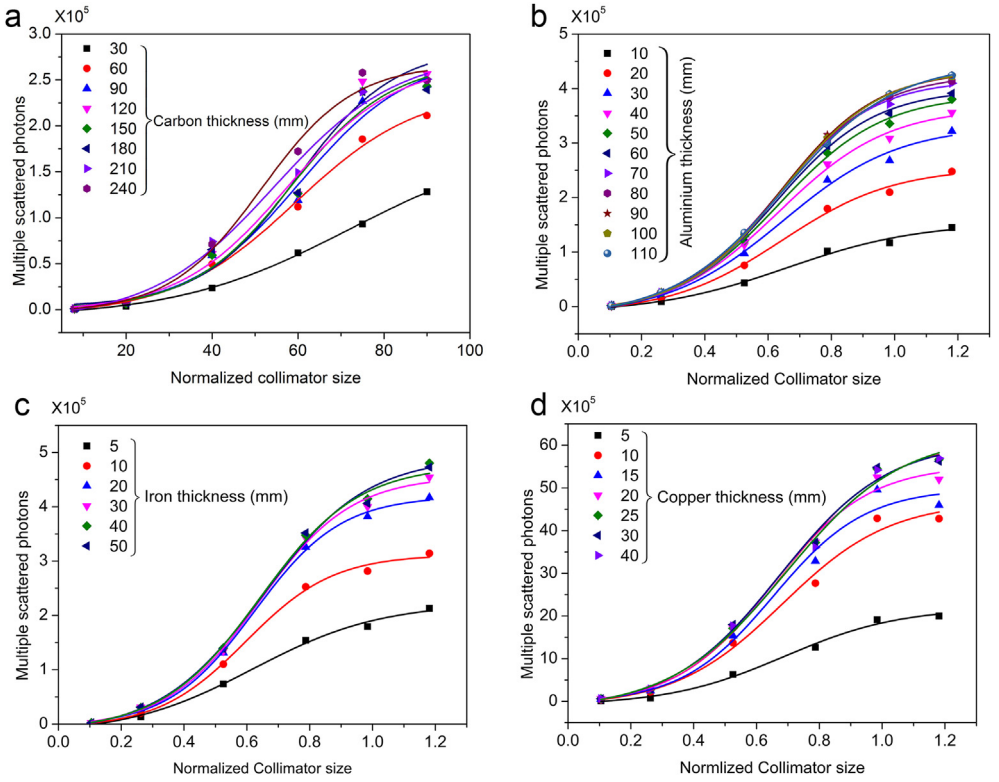

Fig. 7 – Variation of multiple scattered photons as a function of normalized collimator sizes for different target thicknesses.

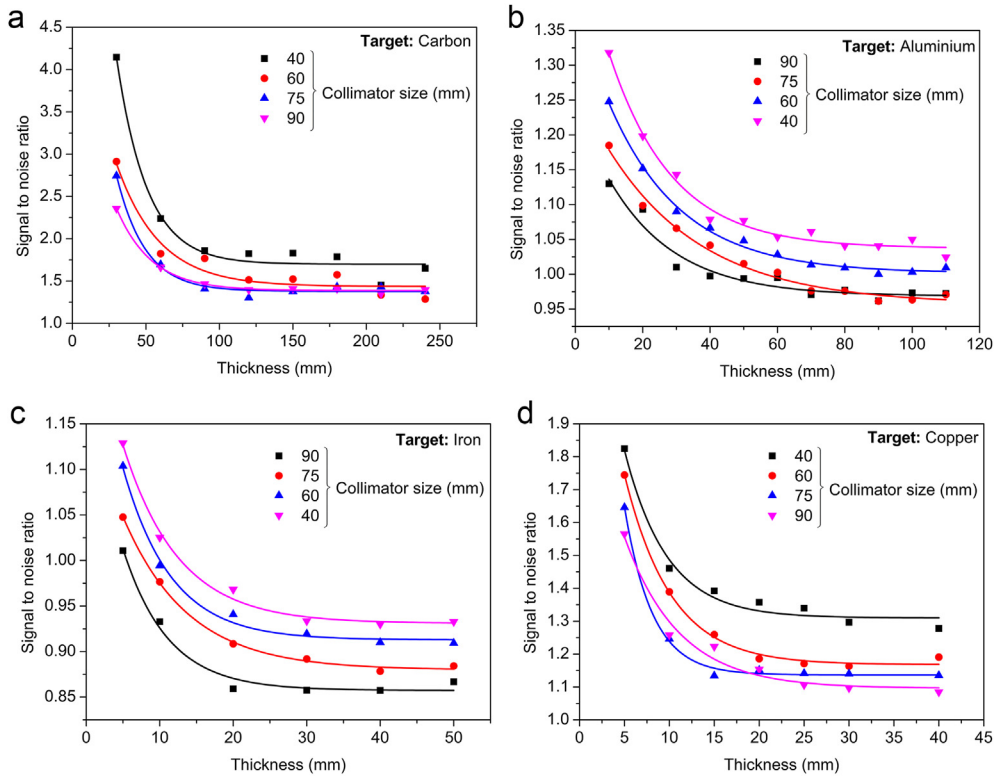

Fig. 8 – Variation of signal-to-noise ratio as a function of target thicknesses for different collimator sizes.

Compton scatter imaging (CSI), a non-destructive examination method used in medical and construction industries. The multiple scatter events contribute a background noise which reduces details and contrast of the image. The influence of the multiple scattered radiation on the quality of the image can be expressed in terms of MSF defined by

$$MSF = \frac{N_m}{N_m + N_s} \tag{6}$$

where N_m and N_s are the multiple and single scattered photons respectively recorded by the gamma detector.

In order to find single scattered photons of the scatterer, it is assumed that the backscattered photons from the target of least thickness (1 mm for Carbon, 2 mm for Aluminium and 3 mm for Iron and Copper) independent of multiple scattering and it is taken as N_s. The MSF as a function of energy window ($\Delta E = 2$ keV) for different collimation sizes and sample thickness is shown in Fig. 9. The plots show that MSF saturates as ΔE increases for different collimator aperture. The increase in MSF value is due to the effect of collimation size, sample thickness and acceptance angle of the gamma detector. The present result agrees well with the Monte Carlo simulation work (Barnea, Dick, Ginzburg, Navon, & Seltzer, 1995).

4.7. *About MCNP simulation*

In order to validate the experimentally obtained values of saturation thicknesses, the entire experimental set-up was simulated using MCNP code and the plot is shown in Fig. 10. MCNP4A (Briesmeister, 1993) radiation transport code is adopted to obtain the saturation thicknesses of various materials. To produce reliable confidence intervals, as many as 15×10^5 histories were run. F1 tally is used to estimate the number of photons crossing front surface of the detector. The results of the simulation are normalized per starting source photon.

5. Conclusions

The present experimental results shows that for thick targets, there is significant contribution of multiple scattered radiation emerging from the scatterer, having energy equal to that of single scattered events. The intensity of multiple scattering increases with increase in target thickness and then saturate at a particular target thickness called saturation thickness. The saturation thickness of the material does not change by the variation in detector collimator opening. The present experimental work shows the dependence of collimator size on Signal-to-Noise ratio and Multiple Scattering Fraction. In order to increase the "signal-to-noise ratio" in Compton profiles, the contribution of multiple scattering background should be minimised which can be achieved by using a narrow detector collimator and thin target thickness. MSF increases and saturates with an increase in energy window around the Compton scattered peak. In order to minimize the MSF value, a narrow detector collimator and/or smaller region of interest in the energy scale is desired. The results of the present work agree well with the available literature (Arvind et al., 2009; Celik et al., 2012; Gurdeep et al., 1999; Sidhu et al., 1999; Singh et al., 2006). The present experimental and simulated work using integrated NaI(Tl) detector on Carbon, Aluminium,

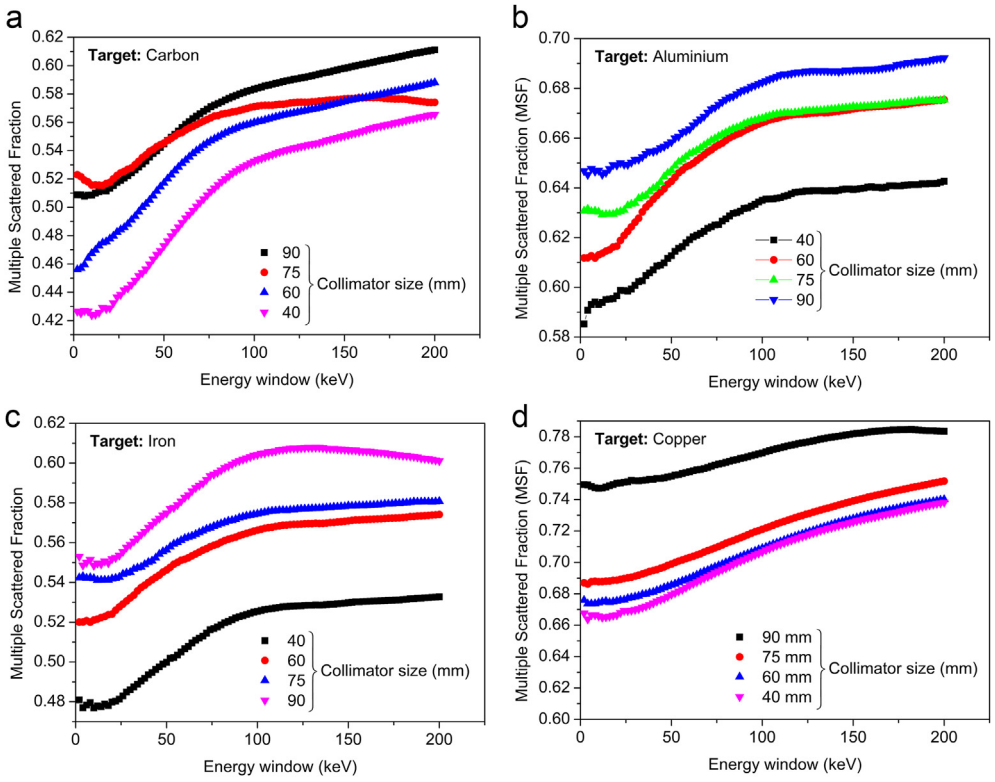

Fig. 9 – A plot of Multiple Scattered Fraction as a function of energy window (2 keV) for different collimator sizes.

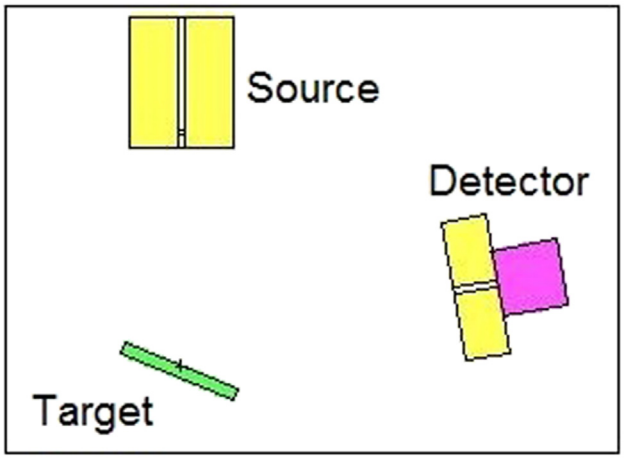

Fig. 10 – MCNP plot of target geometry.

Iron and Copper targets is of the first type and should be a useful reference for *in-situ* measurements.

Acknowledgements

Authors are grateful to University Grants Commission (UGC), Government of India for providing financial assistance in the form of Major Research Project. Thanks to Dr Bhajan Singh and Prof B S Sandhu of Punjabi University, Patiala, India, for their help and guidance throughout the work. K U Kiran is also grateful to UGC for awarding him a fellowship under its Faculty Development Programme. The work was carried out at CARRT, Mangalore University.

REFERENCES

Arvind, D. S., Sandhu, B. S., & Singh, B. (2009). Investigations of effect of target thickness and detector collimation on 662 keV multiply backscattered gamma photons. *Radiation Measurements, 44*, 411–414.

Barnea, G., Dick, C. E., Ginzburg, A., Navon, E., & Seltzer, S. M. (1995). A study of multiple scattering background in Compton scatter imaging. *{NDT} & E International, 28*, 155–162.

Berger, M. J., Hubbell, J. H., Seltzer, S. M., Chang, J., Coursey, J. S., Sukumar, R., et al. (2010). *XCOM: Photon cross section database.* Technical Report 3597. Gaithersburg, MD: National Institute of Standards and Technology.

Bezuidenhout, J. (2013). Measuring naturally occurring uranium in soil and minerals by analysing the 352 keV gamma-ray peak of ^{214}Pb using a NaI(Tl)-detector. *Applied Radiation and Isotopes, 80*, 1–6.

Briesmeister, J. F. (1993). *MCNP a general purpose Monte Carlo N-Particle transport code, version 4A.* Technical Report LA-12625, Los Alamos National Laboratory report.

Celik, N., Cevik, U., & Celik, A. (2012). Effect of detector collimation on the measured mass attenuation coefficients of some elements for 59.5661.6 keV gamma-rays. *Nuclear Instruments and Methods in Physics Research Section B: Beam Interactions with Materials and Atoms, 281*, 8–14.

Costa, J. C., Borger, J. A. R., & Pires, L. F. (2014). Effect of collimator size and absorber thickness on soil bulk density evaluation by gamma-ray attenuation. *Radiation Physics and Chemistry, 95*, 333–335.

Crouthamel, C. E., Adams, F., & Dams, R. (1970). *Applied gamma-ray spectrometry*. Pergamon Press.

Dumond, J. W. M. (1930). Multiple scattering in the Compton effect. *Physical Review, 36*, 1685–1701.

Felsteiner, J., Pattison, P., & Cooper, M. (1974). Effect of multiple scattering on experimental Compton profiles: a Monte Carlo calculation. *Philosophical Magazine, 30*, 537–548.

Golosov, V. N., Walling, D. E., Kvasnikova, E. V., Stukin, E. D., Nikolaev, A. N., & Panin, A. V. (2000). Application of a field-portable scintillation detector for studying the distribution of ^{137}Cs inventories in a small basin in Central Russia. *Journal of Environmental Radioactivity, 48*, 79–94.

Gurdeep, S. S., Karamjit, S., Parjit, S. S., & Gurmel, S. M. (1999). Effect of collimator size and absorber thickness on gamma ray attenuation measurements. *Radiation Physics and Chemistry, 56*, 535–537.

Halonen, V., & Williams, B. (1979). Multiple scattering in the Compton effect. Relativistic cross section for double scattering. *Physical Review B, 19*, 1990–1998.

Jaquiel, S. F., Carlos, R. A., & Avacir, C. A. (2010). Applicability of an X-ray and gamma-ray portable spectrometer for activity measurement of environmental soil samples. *Radiation Measurements, 45*, 801–805.

Kiran, K. U., Ravindraswami, K., Eshwarappa, K. M., & Somashekarappa, H. M. (2014). An investigation of energy dependence on saturation thickness for 59.54, 123, 279, 360, 511, 662, 1115 and 1250 keV gamma photons in carbon and aluminium. *Radiation Physics and Chemistry, 97*(0), 107–112.

Kirkpatrick, P. (1937). Double scattering of polarized X-rays. *Physical Review, 52*, 1201–1209.

Kovler, K., Prilutskiy, Z., Antropov, S., Antropova, N., Bozhko, V., Alfassi, Z. B., et al. (2013). Can scintillation detectors with low spectral resolution accurately determine radionuclides content of building material? *Applied Radiation and Isotopes, 77*, 76–83.

Kwang, H. K., In, S. J., Sung-Woo, K., & Ho-Sik, Y. (2008). Optimum design of detector structure for road transport inspection. *Nuclear Instruments and Methods in Physics Research Section A: Accelerators, Spectrometers, Detectors and Associated Equipment, 591*, 59–62.

Paramesh, L., Venkataramaiah, P., Gopala, K., & Sanjeeviah, H. (1983). Z-dependence of saturation depth for multiple backscattering of 662 keV photons from thick samples. *Nuclear Instruments and Methods in Physics Research, 206*, 327–330.

Pitkanen, T., Cooper, M. J., Laundy, D., & Holt, R. S. (1987). The characterisation of multiple scattering in Compton profile measurements. *Nuclear Instruments and Methods in Physics Research Section A: Accelerators, Spectrometers, Detectors and Associated Equipment, 257*, 384–390.

Plamboeck, A. H., Nylen, T., & Agren, G. (2006). Comparative estimations of ^{137}Cs distribution in a boreal forest in northern Sweden using a traditional sampling approach and a portable NaI detector. *Journal of Environmental Radioactivity, 90*, 100–109.

Povinec, P. P., Osvath, I., & Baxter, M. S. (1996). Underwater gamma-spectrometry with HPGe and NaI(Tl) detectors. *Applied Radiation and Isotopes, 47*, 1127–1133.

Raghunath, V., Bhatnagar, P., & Meenakshisundaram, V. (1983). Non-destructive evaluation of the water content of concretes by low energy gamma backscattering. *Nuclear Instruments and Methods in Physics Research, 206*(12), 303–307.

Ravindraswami, K., Kiran, K. U., Eshwarappa, K. M., & Somashekarappa, H. M. (2014). Non destructive evaluation of selected polymers by multiple scattering of 662 keV gamma rays. *Journal of Radioanalytical and Nuclear Chemistry, 300*(3), 997–1003.

Shengli, N., Jun, Z., & Liuxing, H. (2000). EGS4 simulation of Compton scattering for nondestructive testing. In *KEK Proceedings* (pp. 216–223).

Sidhu, G. S., Singh, K., Singh, P. S., & Mudahar, G. S. (1999). Effect of collimator size and absorber thickness on gamma ray attenuation measurements for bakelite and perspex. *Pramana, 53*, 851–855.

Singh, M., Singh, G., Sandhu, B. S., & Singh, B. (2006). Effect of detector collimator and sample thickness on 0.662 meV multiply Compton-scattered gamma rays. *Applied Radiation and Isotopes, 64*, 373–378.

Singh, G., Singh, M., Sandhu, B. S., & Singh, B. (2007a). Experimental investigation of multiple scattering of 662 keV gamma rays in zinc at 90°. *Radiation Physics and Chemistry, 76*, 750–758.

Singh, M., Singh, G., Sandhu, B. S., & Singh, B. (2007b). Angular distribution of 662 keV multiply-compton scattered gamma rays in copper. *Radiation Measurements, 42*, 420–427.

Singh, G., Singh, M., Sandhu, B. S., & Singh, B. (2008). Experimental investigations of multiple scattering of 662 keV gamma photons in elements and binary alloys. *Applied Radiation and Isotopes, 66*(8), 1151–1159.

Tanner, A. C., & Epstein, I. R. (1976). Multiple scattering in the Compton effect. I. Analytic treatment of angular distributions and total scattering probabilities. *Physical Review A, 13*, 335–348.

Vlachos, D. S., & Tsabaris, C. (2005). Response function calculation of an underwater gamma ray NaI(Tl) spectrometer. *Nuclear Instruments and Methods in Physics Research Section A: Accelerators, Spectrometers, Detectors and Associated Equipment, 539*, 414–420.

Vrba, T., & Fojtik, P. (2014). The design of a NaI(Tl) crystal in a system optimised for high-throughput and emergency measurement of iodine 131 in the human thyroid. *Radiation Physics and Chemistry, 104*(0), 385–388, 1st International Conference on Dosimetry and its Applications.